

# Style-Pro: Style-Guided Prompt Learning for Generalizable Vision-Language Models

Niloufar Alipour Talemi   Hossein Kashiani   Fatemeh Afghah  
Clemson University

{nalipou, hkashia, fafghah}@clemsun.edu

## Abstract

Pre-trained Vision-language (VL) models, such as CLIP, have shown significant generalization ability to downstream tasks, even with minimal fine-tuning. While prompt learning has emerged as an effective strategy to adapt pre-trained VL models for downstream tasks, current approaches frequently encounter severe overfitting to specific downstream data distributions. This overfitting constrains the original behavior of the VL models to generalize to new domains or unseen classes, posing a critical challenge in enhancing the adaptability and generalization of VL models. To address this limitation, we propose Style-Pro, a novel style-guided prompt learning framework that mitigates overfitting and preserves the zero-shot generalization capabilities of CLIP. Style-Pro employs learnable style bases to synthesize diverse distribution shifts, guided by two specialized loss functions that ensure style diversity and content integrity. Then, to minimize discrepancies between unseen domains and the source domain, Style-Pro maps the unseen styles into the known style representation space as a weighted combination of style bases. Moreover, to maintain consistency between the style-shifted prompted model and the original frozen CLIP, Style-Pro introduces consistency constraints to preserve alignment in the learned embeddings, minimizing deviation during adaptation to downstream tasks. Extensive experiments across 11 benchmark datasets demonstrate the effectiveness of Style-Pro, consistently surpassing state-of-the-art methods in various settings, including base-to-new generalization, cross-dataset transfer, and domain generalization.

## 1. Introduction

Vision-language (VL) models like CLIP [33] have exhibited remarkable generalization capabilities across various downstream tasks, including few-shot image recognition [1, 14, 24], object detection [12], and image segmentation [10, 15]. These models are trained on millions of

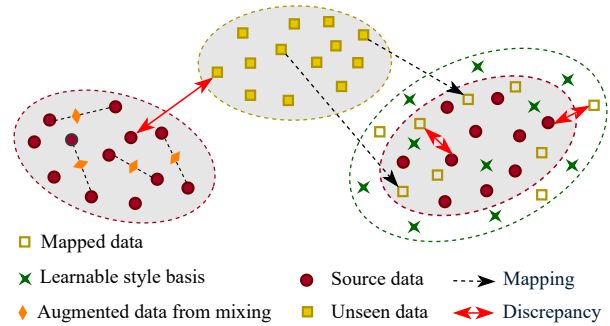


Figure 1. Illustration of the proposed style shift learning approach. Simply mixing feature statistics [43, 50] from the source domain does not generate styles sufficiently distinct from the source domain. Style-Pro addresses this by employing a learnable set of style bases to synthesize style bases beyond the source domain. Furthermore, mapping unseen styles into the style representation space as a weighted combination of these style bases reduces the discrepancy between unseen domains and the source domain.

image-text pairs through contrastive loss, producing a well-aligned joint embedding space for vision and language. For instance, CLIP employs the contrastive learning strategy on a web-scale dataset with 400 million image-text pairs that achieves impressive zero-shot generalization ability by providing text prompts such as “a photo of a [class]”. However, due to their large size, these models can be difficult to fine-tune for smaller tasks, such as few-shot learning, without compromising their generalization capabilities.

One straightforward approach is prompt engineering, where, instead of fine-tuning the entire model, which may result in the loss of valuable knowledge gained during large-scale pre-training, the focus is on identifying effective hand-crafted templates for each task [33]. However, this technique demands considerable manual effort, as designing effective prompts requires deep expert knowledge and substantial time investment. To address this, recent works often incorporate learnable prompts into the text encoder [3, 48, 49], the image encoder [34, 40], or both [22]. In such approaches, the prompts are optimized during train-

ing, while the pre-trained VL models remain unchanged. Prompt learning has become increasingly popular, as it provides an effective way to customize pre-trained VL models for various downstream tasks. Despite advancements in few-shot fine-tuning, optimizing prompts for task-specific objectives often causes the model to overfit to the training samples [22, 48]. This overfitting limits the model’s generalization to new domains or even new classes within the same domain, which has remained a major challenge for adapting the VL models [48].

This work introduces a novel style-guided prompt learning framework called Style-Pro to address the challenges of domain bias in prompt tuning for CLIP. Style-Pro achieves this through two complementary strategies. First, to enhance model generalization and robustness to out-of-distribution (OOD) data, we introduce a style shift learning approach within the prompt-tuning framework. Unlike traditional image-based augmentation methods [7, 19], which often fail to capture a realistic and comprehensive range of domain variations, our proposed approach leverages learnable style bases to extend the diversity of training distribution. In response to the challenges posed by a limited number of samples per class and the lack of samples from target domains, Style-Pro employs two synergistic phases in its style shift learning module. As illustrated in Fig. 1, rather than simply mixing source feature statistics, Style-Pro facilitates the exploration of novel style bases beyond the source distribution during training without requiring additional images. This strategy effectively expands the source domain and minimizes discrepancies between the source and unseen domains. We introduce two new loss functions to synthesize style bases that incorporate various domains while preserving the content information of features. The first one encourages diversity among the style bases by ensuring they spread across a hyperspherical feature space. The second loss function provides the integrity of content information when combining style and content into a new feature. In addition to generating new style bases, Style-Pro maps unseen styles into the style representation space as a weighted combination of style bases (see Fig. 1). The similarity distance between styles serves as the weighting factor, leading to improved adaptability to unseen domains.

Second, to maintain consistency between the style-shifted prompted model and the original frozen CLIP model, Style-Pro enforces alignment by constraining both the text and image encoders. To be more specific, we transfer knowledge from the frozen encoders to the adaptable ones, preserving the robust generalization capabilities of the pre-trained VL model while effectively adapting to a new task within a few-shot learning context. To fully leverage the guidance from the frozen model, we apply two distinct constraints. The first constraint focuses on the difference between the feature representations of the frozen

and prompted encoders, while the second is prediction-based, aiming to improve alignment by fostering synergy between the text and vision encoders. These constraints ensure that the embeddings of the prompted model remain closely aligned with the frozen model, even as it learns new tasks. In summary, the main contributions of this work include:

- We present Style-Pro, a fine-tuning method for CLIP that mitigates overfitting by constraining the prompted model to remain aligned with the frozen CLIP. This approach facilitates efficient learning from limited data while preserving zero-shot generalization capabilities.
- We propose a novel style shift learning approach that synthesizes a diverse range of distinctive styles through learnable style bases. Style-Pro further improves adaptability to unseen domains by representing unseen styles as a weighted combination of these style bases.
- We conduct a comprehensive quantitative analysis on 11 popular image classification benchmarks, demonstrating the effectiveness and robustness of the Style-Pro framework across base-to-novel generalization, cross-dataset transfer, and domain generalization tasks.

## 2. Related Work

### 2.1. Vision-Language Models.

VL models [21, 33, 46] integrate visual and textual modalities to encode comprehensive multi-modal representations. These models are typically pre-trained on extensive datasets; for instance, CLIP [33] and ALIGN [21] are trained on approximately 400 million and 1 billion image-text pairs, respectively. Through self-supervised learning, VL models develop joint image-language representations that significantly enhance their capacity for representation learning. As a result, these models exhibit outstanding performance across a wide range of tasks, including few-shot [4, 28, 30] and zero-shot visual recognition [33]. Nonetheless, adapting these foundational models to specific downstream tasks without diminishing their inherent generalization capabilities remains a significant challenge. In this study, we introduce a novel fine-tuning approach for VL models that mitigates the issue of overfitting and enhances generalization by employing a style-guided prompt learning framework.

### 2.2. Multi-Modal Prompt Tuning for VL Models

Prompt learning has emerged as an efficient technique for fine-tuning large-scale models by integrating learnable embeddings, known as prompt tokens, into the model inputs [9, 28, 48]. Due to its parameter efficiency and fast convergence, prompt learning is a compelling method for

adapting foundational models like CLIP [33] for both vision and VL tasks. CoOp [49] pioneered prompt learning for CLIP by optimizing continuous prompt vectors in its language branch for few-shot image recognition. CoCoOp [48] extends CoOp by improving generalization through conditioning text prompts on visual features. MaPLe [22] further advances this by introducing a multi-modal prompt tuning framework that enhances transferability through the joint learning of hierarchical prompts across both the vision and language branches. Despite recent advances, prompt learning approaches still struggle with overfitting. To address this, we fine-tune learnable prompts using a novel consistency-based alignment that incorporates an innovative style shift learning approach, enhancing generalizability without relying on external data.

### 2.3. Consistency Regularization

Regularization techniques, including weight decay [27], dropout [39], and data augmentation [5] are widely employed to prevent overfitting and enhance generalization to new data [26]. A recent study, CoPrompt [37], proposes a consistency regularization technique to improve the generalizability of the model by aligning the features between the prompted and frozen CLIP. However, this approach fails to account for the essential synergy between the visual and textual domains. Our approach addresses this by not only aligning feature-based consistency but also the cross-modal outputs of the prompted and frozen CLIP, strengthening the interaction between text and vision encoders. Additionally, we introduce a style shift learning technique instead of image-level perturbations [37], enhancing generalization capability across diverse styles without incurring computational overhead.

## 3. Method

### 3.1. Preliminaries

**Contrastive Language-Image Pre-training (CLIP).** CLIP [33] has demonstrated a robust capability to learn open-set visual concepts. This model utilizes visual and textual encoders to produce corresponding embeddings from a given image and its associated textual description. Let  $f(\cdot)$  and  $g(\cdot)$  represent the image encoder and text encoder of CLIP, respectively. Their pre-trained parameters are denoted as  $\theta_{CLIP} = \theta_f, \theta_g$ , where  $\theta_f$  refers to the image encoder parameters and  $\theta_g$  refers to the text encoder parameters. For a given image  $X$ , the extraction of image features begins by dividing the image into  $\mathbf{P}^2$  patches. These patches are then processed through a projection operation known as PatchEmbed, which splits the input image into fixed-size patches and projects them into the feature space. Subsequently, a learnable class token  $CLS$  is concatenated with these features, forming the sequence

$\tilde{X} = \{CLS, e_1, e_2, \dots, e_{\mathbf{P}^2}\}$ . This sequence is then passed through  $L$  transformer layers to generate the visual feature representation,  $\tilde{\mathbf{f}} \in \mathbb{R}^d$ . Similarly, given the class name of the  $i^{th}$  class, denoted as  $y$ , the WordEmbed component first transforms the hand-crafted description, such as "a photo of a class name," into a sequence of vectorized textual tokens. This sequence can be represented as  $\tilde{Y} = \{t_{SOS}, t_1, t_2, \dots, t_T, c_k, t_{EOS}\}$ , where  $c_k$  is the word embedding corresponding to the class label, and  $t_{SOS}$  and  $t_{EOS}$  are learnable start and end tokens, respectively. The text encoder  $g$  encodes  $\tilde{Y}$  via multiple transformer layers to produce the latent text feature,  $\tilde{\mathbf{g}} \in \mathbb{R}^d$ . For zero-shot inference, text features of the text template with class labels  $\{1, 2, \dots, C\}$  are matched with the image feature as  $\frac{\exp(\text{sim}(\tilde{\mathbf{g}}_i, \tilde{\mathbf{f}})/\tau)}{\sum_{i=1}^C \exp(\text{sim}(\tilde{\mathbf{g}}_i, \tilde{\mathbf{f}})/\tau)}$ , where  $\text{sim}(\cdot)$  denotes the cosine similarity and  $\tau$  is the temperature.

**Prompt Learning.** Inspired by prompt learning in NLP, numerous studies have explored the VL models by incorporating learnable prompt tokens during end-to-end training. In this study, we utilize hierarchical learnable prompt tokens independently for the text and image encoders, following the simple baseline method called Independent Vision-Language Prompting (IVLP) [35]. We concatenate learnable language prompts, denoted as  $P_t = \{p_t^1, p_t^2, \dots, p_t^T\}$ , and visual prompts, denoted as  $P_v = \{p_v^1, p_v^2, \dots, p_v^V\}$ , into the respective sets of textual and visual input tokens. Thus, the image encoder generates the prompted visual feature  $\tilde{\mathbf{f}}_p = f(\tilde{X}_p, \theta_f)$  from input tokens  $\tilde{X}_p = \{P_v, e_{CLS}, e_1, e_2, \dots, e_{\mathbf{P}^2}\}$ , and the textual feature  $\tilde{\mathbf{g}}_p = g(\tilde{Y}_p, \theta_g)$  is obtained from  $\tilde{Y}_p = \{t_{SOS}, P_t, t_1, t_2, \dots, t_T, c_k, t_{EOS}\}$ . It should be noted that in this work, we employ deep prompting, which involves learning distinct sets of prompts for each transformer layer. For image classification on a downstream dataset  $D_s$ , prompts interact with frozen  $\theta_f$  and  $\theta_g$  and are optimized with the cross-entropy loss as:

$$\mathcal{L}_{CE} = \frac{1}{N} \sum_{(X,y) \in \mathcal{D}_s} \frac{\exp(\text{sim}(\tilde{\mathbf{f}}_p, \tilde{\mathbf{g}}_y)/\tau)}{\sum_{i=1}^C \exp(\text{sim}(\tilde{\mathbf{f}}_p, \tilde{\mathbf{g}}_i)/\tau)}. \quad (1)$$

### 3.2. Style-Guided Prompt Learning

Fig. 2 presents an overview of the Style-Pro framework. This framework integrates two complementary strategies: style shift learning and consistency constraints. Style-Pro incorporates an innovative style shift learning strategy to synthesize diverse style shifts and enhance robustness against OOD data. In parallel, Style-Pro introduces consistency constraints to preserve the alignment of the embeddings between the style-shifted prompted model and the pre-trained frozen CLIP, minimizing deviation during adaptation to downstream tasks.

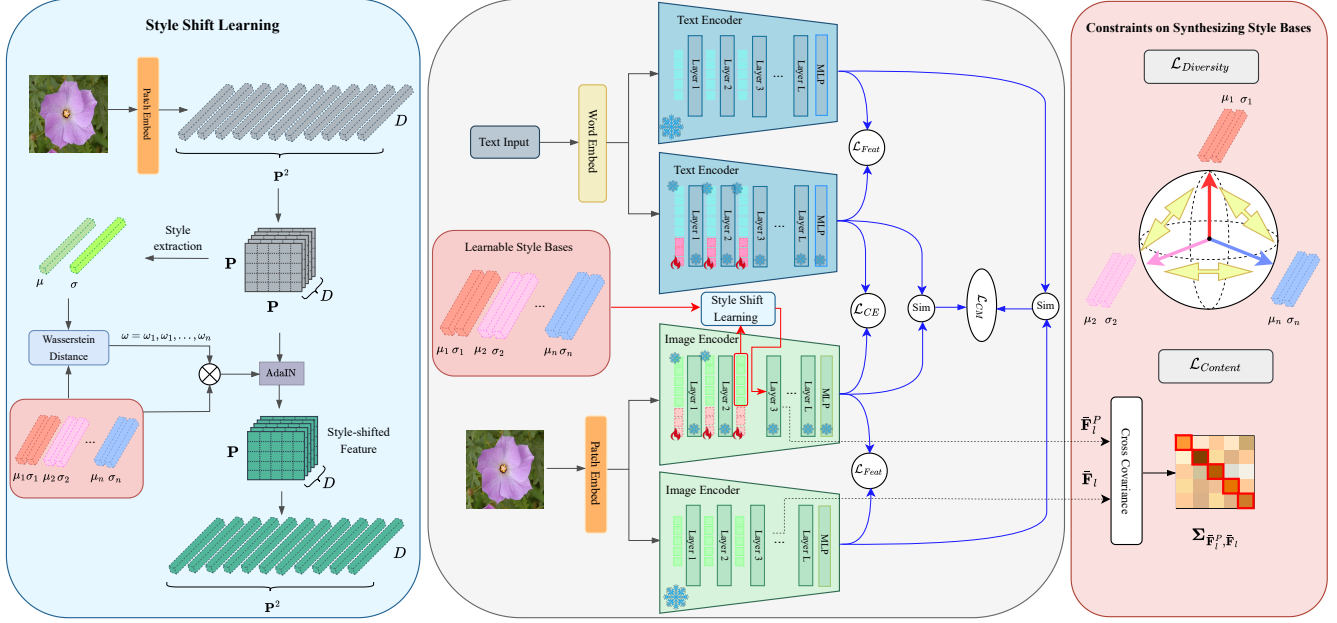


Figure 2. Overview of the proposed Style-Pro framework. Style-Pro introduces a style-guided prompt learning framework, incorporating a novel style shift learning approach in the feature space through a learnable set of style bases. Unseen styles are mapped into the style representation space as a weighted combination of style bases, reducing style discrepancies and improving performance on OOD data. Furthermore, Style-Pro ensures consistency between the embeddings of the prompted and frozen models during adaptation, which facilitates fine-tuning of CLIP while preserving its generalization capabilities.

**Style Shift Learning.** Adapting CLIP to downstream tasks often compromises OOD performance, as prompt learning is restricted to the training data distribution. To tackle the challenge of handling arbitrary unseen domains during testing, it is crucial to reduce the style discrepancies between training and test distributions. Our framework introduces a novel style shift learning approach using a learnable set of style bases, which addresses this issue more effectively than traditional image-based augmentation methods [7, 19]. This approach is computationally efficient and covers a broader range of styles beyond the source distribution without additional images.

Several studies [20, 50] have demonstrated that the shallow feature distribution of networks can reflect the style information of the input image. For a feature map  $\mathbf{F} \in \mathbb{R}^{h \times w \times c}$ , AdaIN [20] shows that the channel-wise mean  $\mu \in \mathbb{R}^c$  and standard deviation  $\sigma \in \mathbb{R}^c$  convey information about the style of the input image. Therefore, stylizing a given feature  $\mathbf{F}$  with an arbitrary target style  $(\mu_t, \sigma_t)$  is performed as follows:

$$\text{AdaIN}(\mathbf{F}, \mu_t, \sigma_t) = \sigma_t \left( \frac{\mathbf{F} - \mu(\mathbf{F})}{\sigma(\mathbf{F})} \right) + \mu_t, \quad (2)$$

where  $\mu(\cdot)$  and  $\sigma(\cdot)$  denote the mean and standard deviation of the input feature, respectively.

Given an input image, as discussed in Section 3.1, the  $l$ -th layer of ViT generates  $\mathbf{P}^2 + 1$  token representations.

Among these,  $\mathbf{P}^2$  representations are derived from the image patches, and one of them corresponds to the learnable classification token ( $\mathbf{F}_l \in \mathbb{R}^{(\mathbf{P}^2+1) \times D}$ ), where  $D$  represents the dimension of each token representation. To extract the style information from the  $l$ -th layer of ViT, following the methodology established by [13], we employ AdaIN across the dimension of the token representations. As illustrated in Fig. 2, this process involves reshaping the patch representations into  $\mathbf{F}'_l \in \mathbb{R}^{\mathbf{P} \times \mathbf{P} \times D}$ . Subsequently, we can calculate the style information for the token representations as follows;

$$\mu(\mathbf{F}'_l) = \frac{1}{\mathbf{P}^2} \sum_{k=1}^{\mathbf{P}} \sum_{k=1}^{\mathbf{P}} \mathbf{F}'_l, \quad (3)$$

$$\sigma(\mathbf{F}'_l) = \sqrt{\frac{1}{\mathbf{P}^2} \sum_{k=1}^{\mathbf{P}} \sum_{k=1}^{\mathbf{P}} (\mathbf{F}'_l - \mu(\mathbf{F}'_l))^2 + \epsilon}, \quad (4)$$

where  $\mu(\mathbf{F}'_l), \sigma(\mathbf{F}'_l) \in \mathbb{R}^D$ . Considering a collection of style bases  $B_{sty} = (\mu_b^n, \sigma_b^n)_{n=1}^N$ , we enhance the styles of training features to improve the generalization ability to new domains. Initially, we compute the Wasserstein distance [41] to determine the discrepancy in style distribution between the current image  $(\mu_{cur}, \sigma_{cur})$  and the  $n$ -th style basis  $(\mu_b^n, \sigma_b^n)$  as follows:

$$d_{cur} = \|\mu_{cur} - \mu_b^n\|_2^2 + (\sigma_{cur}^2 + \sigma_b^{n2} - 2\sigma_{cur}\sigma_b^n). \quad (5)$$

Next, the reciprocal of  $d_{cur}$  is used to measure the similarity between the current image and the  $n$ -th style basis:

$$\omega_n = \frac{\exp(1/(1 + d_{cur}))}{\sum_{n=1}^N \exp(1/(1 + d_{cur}))}, \quad (6)$$

where the softmax function ensures that the sum of  $\omega = \omega_n | n = 1, 2, \dots, N$  equals 1. Based on the estimated similarity  $\omega$ , the mapped style  $(\mu_{map}, \sigma_{map})$  is obtained by the weighted sum of the style bases:

$$\mu_{map} = \sum_{n=1}^N \omega_n \mu_b^n, \quad \sigma_{map} = \sum_{n=1}^N \omega_n \sigma_b^n. \quad (7)$$

Therefore, the style bases most similar to the unseen style play a more dominant role in mapping the unseen style. Finally, using Eq. 2, the mapped style is applied to the normalized feature  $(\bar{\mathbf{F}}'_l)$  to obtain the style-shifted feature  $(\mathbf{F}''_l)$  as follows:

$$\mathbf{F}''_l = \sigma_{map} \bar{\mathbf{F}}'_l + \mu_{map}. \quad (8)$$

Following this operation, the style-shifted token representations are fed into the subsequent layer of the prompted encoder.

**Constraints on Synthesizing Styles.** To address the various domain shifts, our proposed method adheres to two constraints to produce optimized and efficient style bases. The first constraint ensures that the synthesized styles comprehensively cover the feature space, thereby enhancing the ability of the model to generalize across different domains. To achieve this, we employ a novel loss function that compels the model to generate a diverse set of styles, each representing different points on the hyper-sphere. To maximize the diversity of  $N$  style bases in a hyper-spherical feature space, each style basis must be orthogonal to all other style bases. Consequently, we minimize the absolute value of the cosine similarity between the  $n$ -th style basis and every other existing style basis, as expressed by the following equation:

$$\mathcal{L}_{Diversity} = \sum_{n=1}^N \left( \sum_{\substack{k=1 \\ k \neq n}}^N \left| \frac{\mu_b^n}{\|\mu_b^n\|} \cdot \frac{\mu_b^k}{\|\mu_b^k\|} \right| + \sum_{\substack{k=1 \\ k \neq n}}^N \left| \frac{\sigma_b^n}{\|\sigma_b^n\|} \cdot \frac{\sigma_b^k}{\|\sigma_b^k\|} \right| \right). \quad (9)$$

Focusing only on the diversity constraint is insufficient for synthesizing appropriate style bases. It is important to have diverse styles that do not damage the content information of the features. This requires that in each layer, features from both the prompted and frozen vision encoders convey identical content. Imposing this constraint ensures that the model preserves content consistency when shifting styles in the prompted vision encoder. Given the normalized features,  $\bar{\mathbf{F}}'_l$  and  $\bar{\mathbf{F}}_l$ , from the  $l$ -th layer of the prompted and

frozen vision encoders, respectively, the cross-covariance matrix is computed as follows:

$$\Sigma_{\bar{\mathbf{F}}'_l, \bar{\mathbf{F}}_l} = \mathbf{E}[\bar{\mathbf{F}}'_l \cdot (\bar{\mathbf{F}}_l)^T]. \quad (10)$$

Since  $\bar{\mathbf{F}}'_l$  and  $\bar{\mathbf{F}}_l$  should contain identical content, the diagonal elements of their cross-covariance matrix are expected to be equal to 1 [47]. Consequently, we define the content consistency loss as follows:

$$\mathcal{L}_{Content} = \|\text{diag}(\Sigma_{\bar{\mathbf{F}}'_l, \bar{\mathbf{F}}_l}) - \mathbf{1}\|_2, \quad (11)$$

where  $\text{diag}() \in \mathbb{R}^D$  denotes the column vector comprising diagonal elements of  $\Sigma_{\bar{\mathbf{F}}'_l, \bar{\mathbf{F}}_l}$  and  $\mathbf{1} \in \mathbb{R}^D$  denotes the one vector.

**Self-Consistency Regularization.** As outlined in the previous subsection, merely training prompts with a supervised task-specific loss does not adequately preserve the general attributes inherent in the frozen CLIP. Consequently, despite keeping the weights of the CLIP image and text encoders fixed, their performance on new tasks deteriorates. To overcome this limitation, we propose a novel regularization method that ensures the prompted model maintains its generalization capability across new classes and diverse domains. This is accomplished by applying complementary constraints, which allow CLIP to retain its general knowledge while learning prompts for downstream tasks.

To effectively leverage the guidance of the frozen model, it is crucial to minimize the variations introduced by the prompts across different modality branches. To this end, we impose two distinct constraints on the prompted visual and textual features to ensure their alignment with the frozen CLIP features. For a given input sample and its corresponding textual label, we extract textual and visual features using both the prompted and frozen latent spaces. Subsequently, we apply the following two complementary loss functions:

• **Feature-level Alignment.** To evaluate the similarity between feature representations, we utilize the Mean Square Error (MSE) as a metric to quantify the average squared differences. This approach accurately assesses how closely the predicted embeddings align with the frozen model embeddings. The loss function is defined as:

$$\mathcal{L}_{Feat} = \frac{1}{d} \left( \lambda_f \sum_{i=1}^d (\tilde{\mathbf{f}}_i - \tilde{\mathbf{f}}_{p_i})^2 + \lambda_g \sum_{i=1}^d (\tilde{\mathbf{g}}_i - \tilde{\mathbf{g}}_{p_i})^2 \right), \quad (12)$$

where  $\tilde{\mathbf{f}}_{p_i}$  and  $\tilde{\mathbf{g}}_{p_i} \in \mathbb{R}^d$  represent the vision and text embeddings derived from the prompted model, respectively. The parameters  $\lambda_f$  and  $\lambda_g$  are weighting factors that control the contribution of the vision and text modalities to the overall loss.

• **Cross-modality Alignment.** The performance of VL models can degrade substantially when there is a misalignment between the visual and textual domains. These discrepancies often arise due to inherent differences in how visual and textual data are represented and processed within these models. To tackle this challenge and enhance the integration between the text and vision-prompted encoders, we further align the output predictions of the prompted model ( $Pre_p$ ) with those of the pre-trained frozen CLIP ( $Pre$ ) by employing Kullback-Leibler (KL) divergence. Specifically, we define the cross-modality alignment loss as:

$$\mathcal{L}_{CM} = \mathcal{D}_{KL}(Pre, Pre_p), \quad (13)$$

$$Pre = \text{sim}(\tilde{f}, \tilde{g}), \quad Pre_p = \text{sim}(\tilde{f}_p, \tilde{g}_p), \quad (14)$$

where the function  $\text{sim}()$  represents cosine similarity. This alignment enables the model to achieve a comprehensive understanding of both visual and textual information. As a result, our method enhances the generalization performance across diverse domains, mitigating the risk of performance degradation due to discrepancies between the text and vision modalities.

We utilize the weighted combination of all the mentioned loss terms for the end-to-end training. Therefore, our final loss function is:

$$\mathcal{L}_{total} = \mathcal{L}_{CE} + \mathcal{L}_{CM} + \mathcal{L}_{Feat} + \lambda_1 \mathcal{L}_{Diversity} + \lambda_2 \mathcal{L}_{Content}, \quad (15)$$

where  $\lambda_1$  and  $\lambda_2$  are hyperparameters that control the relative importance of the diversity and content losses, respectively.

## 4. Experiments

### 4.1. Datasets and Implementation Details

Following previous prompt tuning studies [22, 35, 48], we validate our method across three different settings: generalization from base-to-novel classes, cross-dataset evaluation, and domain generalization. Our experiments incorporate a variety of datasets, including two generic-object datasets (ImageNet [8] and Caltech101 [11]), fine-grained datasets (OxfordPets [32], StanfordCars [25], Flowers102 [31], Food101 [2], and FGVC Aircraft [29]), a remote sensing classification dataset (EuroSAT [16]), a scene recognition dataset (SUN397 [44]), an action recognition dataset (UCF101 [38]), and a texture dataset (DTD [6]). For domain generalization, we employ ImageNet as the source dataset, and its four variants as target datasets, including ImageNetV2 [36], ImageNetSketch [42], ImageNet-A [18], and ImageNet-R [17]. All these experiments are conducted

using a 16-shot setting, meaning that only 16 training examples are provided for each category.

In our experiments, we utilize a ViT-B/16-based CLIP model, employing deep prompting with  $V = T = 4$  VL prompts. It should be noted that the prompts are randomly initialized using a normal distribution, except for the text prompts in the first layer, which are initialized with the word embeddings of “a photo of a”. For domain generalization and cross-dataset evaluation, learnable prompts are injected into the first three transformer layers. In the base-to-novel setting, prompts are injected into the first nine transformer layers. Each model is trained for 25 epochs with a batch size of 4 and a learning rate of 0.0025 using the SGD optimizer on a single NVIDIA RTX 4090 GPU. The results are averaged over three runs. We set the parameters  $\lambda_f$  and  $\lambda_g$  in  $\mathcal{L}_{MSE}$  to 15 and 25, respectively. The diversity loss  $\mathcal{L}_{diversity}$  and the content loss  $\mathcal{L}_{content}$  are weighted by factors of 0.005 and 0.2, respectively. The number of style bases,  $N$ , is fixed at 12 for all experiments.

### 4.2. Base-to-Novel Generalization

To evaluate the generalization capability of our method within a dataset, we conduct evaluations on 11 different image classification datasets. Adhering to the experimental setup established by previous studies [22, 28, 48], each dataset is divided into base and novel classes. The model is trained on the base classes utilizing a few-shot learning approach with 16 shots and is subsequently evaluated on both the base and novel classes. The results, presented in Table 1, compare our proposed method with state-of-the-art techniques, including Zero-shot CLIP [33], CoOp [49], Co-CoOp [48], MaPLe [22], CoPrompt [37], PromptSRC [23], and MMA [45], across the 11 datasets. Notably, Style-Pro demonstrates exceptional performance in addressing one of the most challenging categories, unseen classes, underscoring its superior zero-shot generalizability to novel scenarios. Specifically, our Style-Pro achieves a 0.83% average gain over CoPrompt [37] on novel class generalization. It is also important to highlight that while Style-Pro surpasses its competitors in handling new classes, it maintains effective adaptation to base classes with an average 0.22% improvement over the second-best result. Although a few methods marginally outperform Style-Pro in specific base classes, the difference is negligible. These results highlight the robustness of Style-Pro in adapting to downstream tasks while still maintaining strong generalization ability.

### 4.3. Cross-Dataset Evaluation

In cross-dataset evaluation, similar to the state-of-the-art methods [28, 37, 48], we train the model on ImageNet [8] and directly evaluate it on other datasets without any data-specific fine-tuning. Table 3 summarizes the results of our cross-dataset evaluation. Style-Pro demonstrates an average

improvement of 0.24% over existing methods, consistently outperforming them across various datasets. This strong performance highlights the good zero-shot transferability of the proposed Style-Pro, making it highly suitable for applications requiring adaptability across diverse datasets.

#### 4.4. Domain Generalization

Table 2 presents a summary of the results for Style-Pro in comparison with previous methods on OOD datasets. In line with prior works [28, 37, 37, 45, 48], we fine-tune our model on ImageNet dataset [8] and evaluate it on several ImageNet variants. As shown in Table 2, our approach consistently outperforms existing methods in terms of robustness to domain shifts within the domain generalization setting. This demonstrates that style shift learning enables the model to map the styles of unknown domains into a dedicated style representation space, thus minimizing discrepancies in style and improving performance on OOD datasets.

#### 4.5. Ablation and Analysis

In this subsection, we assess the individual contributions of each component of the proposed Style-Pro framework. We demonstrate how these components complement each other to mitigate overfitting in VL model adaptation, leading to improved generalization performance.

**Effectiveness of each constraint.** Table 4 summarizes the results of the ablation study on the various constraints introduced in our Style-Pro framework, with the outcomes averaged over 11 datasets. To elucidate the impact of our alignment constraints, we conduct two distinct experiments. The first experiment considers only the feature-level constraint (second row), while the second incorporates both the feature-level and the cross-modality alignment (third row). We compare the performance of these approaches with the baseline approach, which utilizes only IVLP (first row). The results demonstrate that applying both constraints together enhances accuracy for both base and new classes, thereby confirming its effectiveness in improving generalizability. Additionally, we implement two further experiments to assess the impact of our style shift learning approach on the accuracy improvement of the VL model. The results (see Table 4) indicate that incorporating content loss, which preserves the content information of style-shifted features, enhances the model’s ability to discriminate effectively (as shown in the fourth row). Moreover, enforcing a broader range of synthetic style bases significantly boosts accuracy for both base and new classes (the fifth row), with a particularly notable improvement observed in the new classes, aligning with our primary objective.

**Analysis of different augmentation approaches for the prompted vision encoder.** To further illustrate the impact of our proposed style shift learning approach, we com-

Dataset	CLIP [33]	CoOp [49]	CoCoOp [48]	MaPLe [22]	PromptSRC [23]	CoPrompt [37]	MMA [45]	Style-Pro (Proposed)
Average on 11 datasets	B 69.34	82.69	80.47	82.28	84.26	84.00	83.20	<b>84.48</b>
	N 74.22	63.22	71.69	75.14	76.10	77.23	76.80	<b>78.06</b>
	H 71.70	71.66	75.83	78.55	79.97	80.48	79.87	<b>80.98</b>
ImageNet	B 72.43	76.47	75.98	76.66	77.60	<b>77.67</b>	77.31	77.58
	N 68.14	67.88	70.43	70.54	70.73	71.27	71.00	<b>71.68</b>
	H 70.22	71.92	73.10	73.47	74.01	74.33	74.02	<b>74.51</b>
Caltech101	B 96.84	98.00	97.96	97.74	98.10	98.27	<b>98.40</b>	98.38
	N 94.00	89.81	93.81	94.36	94.03	94.90	94.00	<b>95.44</b>
	H 95.40	93.73	95.84	96.02	96.02	96.55	96.15	<b>96.89</b>
OxfordPets	B 91.17	93.67	95.20	95.43	95.33	<b>95.67</b>	95.40	95.64
	N 97.26	95.29	97.69	97.76	97.30	98.10	98.07	<b>98.63</b>
	H 94.12	94.47	96.43	96.58	96.30	96.87	96.72	<b>97.11</b>
Stanford Cars	B 63.37	78.12	70.49	72.94	78.27	76.97	78.50	<b>78.53</b>
	N 68.65	60.40	73.59	74.00	74.97	74.40	73.10	<b>75.12</b>
	H 68.65	68.13	72.01	73.47	76.58	75.66	75.70	<b>76.79</b>
Flowers 102	B 72.08	97.60	94.87	95.92	<b>98.07</b>	97.27	97.77	98.04
	N 77.80	59.67	71.75	72.46	76.50	76.60	75.93	<b>76.86</b>
	H 74.83	74.06	81.71	82.56	85.95	85.71	85.48	<b>86.17</b>
Food101	B 92.43	88.33	90.70	90.71	90.67	90.73	90.13	<b>90.93</b>
	N 91.22	82.26	91.29	92.05	91.53	92.07	91.30	<b>92.29</b>
	H 90.66	85.19	90.99	91.38	91.10	91.40	90.71	<b>91.60</b>
FGVC Aircraft	B 27.19	40.44	33.41	37.44	42.73	40.20	40.57	<b>42.79</b>
	N 36.29	22.30	23.71	35.61	37.87	<b>39.33</b>	36.33	39.28
SUN397	B 69.36	80.60	79.74	80.82	<b>82.67</b>	82.63	82.27	82.66
	N 75.35	65.89	76.86	78.70	78.47	80.03	78.57	<b>80.61</b>
	H 72.23	72.51	78.27	79.75	80.52	81.31	80.38	<b>81.62</b>
DTD	B 53.24	79.44	77.01	80.36	83.37	83.13	83.20	<b>83.41</b>
	N 59.90	41.18	56.00	59.18	62.97	64.73	<b>65.63</b>	65.58
	H 56.37	54.24	64.85	68.16	71.75	72.79	73.38	<b>73.43</b>
EuroSAT	B 56.48	92.19	87.49	94.07	92.90	<b>94.60</b>	85.46	94.52
	N 64.05	54.74	60.04	73.23	73.90	78.57	82.34	<b>82.74</b>
	H 60.03	68.69	71.21	82.35	82.32	85.84	83.87	<b>88.24</b>
UCF101	B 70.53	84.69	82.33	83.00	87.10	<b>86.90</b>	86.23	86.83
	N 77.50	56.05	73.45	78.66	78.80	79.57	80.03	<b>80.40</b>
	H 73.85	67.46	77.64	80.77	82.74	83.07	82.20	<b>83.49</b>

Table 1. Comparison of our proposed method with state-of-the-art methods on different datasets in the base-to-novel generalization setting. ‘B’ and ‘N’ denote accuracy on base and novel classes, respectively. ‘H’ represents the harmonic mean of base and novel accuracy, reflecting the balance between adaptation and generalization.

	Source	Target				
	ImageNet	-V2	-S	-A	-R	Avg.
CLIP [33]	66.73	60.83	46.15	47.77	73.96	57.18
CoOp [49]	71.51	64.20	47.99	49.71	75.21	59.28
CoCoOp [48]	71.02	64.07	48.75	50.63	76.18	59.91
MaPLe [22]	70.72	64.07	49.15	50.90	76.98	60.27
PromptSRC [23]	<b>71.27</b>	64.35	49.55	50.90	77.80	60.65
CoPrompt [37]	70.80	64.81	49.54	51.51	77.34	60.80
MMA [45]	71.00	64.33	49.13	51.12	77.32	60.77
Style-Pro	71.23	<b>65.66</b>	<b>50.38</b>	<b>51.93</b>	<b>77.98</b>	<b>61.49</b>

Table 2. Comparison of our proposed method with state-of-the-art studies in the domain generalization setting.

pare its performance with alternative augmentation methods. As shown in Table 5, replacing our method with standard image-based augmentations, such as random resized cropping (second row), or a more advanced technique like

	Source	Target										
	ImageNet	Caltech101	OxfordPets	StanfordCars	Flowers102	Food101	Aircraft	SUN397	DTD	EuroSAT	UCF101	Average
CoOp [49]	71.51	93.70	89.14	64.51	68.71	85.30	18.47	64.15	41.92	46.39	66.55	63.88
CoCoOp [48]	71.02	94.43	90.14	65.32	71.88	86.06	22.94	67.36	45.73	45.37	68.21	65.74
MaPLe [22]	70.72	93.53	90.49	65.57	72.23	86.20	24.74	67.01	46.49	48.06	68.69	66.30
PromptSCR [23]	<b>71.27</b>	93.60	90.25	65.70	70.25	86.15	23.90	67.10	46.87	45.50	68.75	65.81
CoPrompt [37]	70.80	94.50	90.73	65.67	72.30	86.43	24.00	67.57	47.07	<b>51.90</b>	69.73	67.00
MMA [45]	71.00	93.80	90.30	<b>66.13</b>	72.07	86.12	<b>25.33</b>	68.17	46.57	49.24	68.32	66.61
Style-Pro	71.23	<b>94.66</b>	<b>90.91</b>	66.03	<b>72.54</b>	<b>86.61</b>	25.14	<b>68.38</b>	<b>47.29</b>	50.85	<b>69.96</b>	<b>67.24</b>

Table 3. Comparison of our proposed method with state-of-the-art approaches in cross-dataset evaluation. Our method achieves superior average performance across 10 datasets, highlighting its strong zero-shot adaptability.

Approach		Accuracy		
Consistency	Style Shift	Base	Novel	HM
		82.51	73.36	77.66
✓		82.77	74.28	78.30
✓	✓	82.97	75.64	79.14
✓	✓	83.11	76.09	79.45
✓	✓	<b>84.48</b>	<b>78.06</b>	<b>80.98</b>

Table 4. Analysis of different constraints of Style-Pro framework.

RandAugment [7] (third row), does not yield significant improvements over the baseline model without any augmentation (first row). Furthermore, we explore the application of MixStyle [50] as a substitute for our approach. Although MixStyle as a feature-level augmentation method demonstrates some performance gains, the results clearly indicate that our proposed approach substantially outperforms all other strategies. This highlights the superiority of our approach in boosting the generalization capacity of the model.

**Analysis of the number of style bases and the layer selection for style shift learning.** Fig. 3 (a) explores the effects of applying style shift learning at different layers of the vision encoder. The results indicate that applying style shift learning at the second layer achieves the optimal balance in accuracy across the base, novel, and HM categories, highlighting this layer as the most effective for integrating style variations. Subsequently, we examine the influence of the number of learnable style bases, as shown in Fig. 3 (b). The curves reveal that a limited number of style bases fails to address the broad spectrum of domain shifts, resulting in poor generalization, while too many bases add unnecessary complexity, reducing performance. Thus, we set the number of style bases to 12 in all experiments.

## 5. Conclusion

In this work, we present a style-guided prompt learning framework for fine-tuning VL models in the context

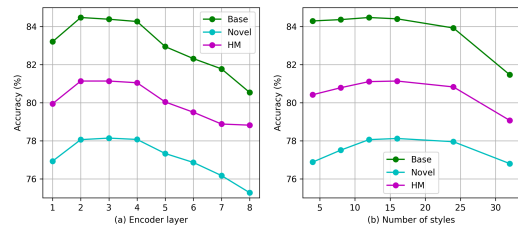


Figure 3. (a) Ablation study on style shift learning at different layers of the vision encoder. (b) Ablation study on the impact of the number of learnable style bases.

Approach	Accuracy (HM)
Baseline	79.14
Simple Augmentation	79.81
RandAugment [7]	79.75
MixStyle [50]	79.93
Style-Pro	<b>80.98</b>

Table 5. Analysis of different augmentation approaches for the vision encoder.

of few-shot image recognition. Our framework leverages a novel style shift learning approach that enhances the model’s robustness to OOD data by utilizing learnable style bases. Further, we maintain alignment between the style-shifted prompted model and the frozen pre-trained CLIP, ensuring the frozen model’s generalization capacity is preserved while fine-tuning for downstream tasks. Extensive experiments on 11 image classification benchmarks demonstrate that Style-Pro consistently outperforms existing methods, with more considerable gains in generalization to new classes and domains.

## Acknowledgment

This material is based upon work supported by the National Science Foundation under Grant Numbers CNS-2232048, and CNS-2204445.



## References

- [1] Shirsha Bose, Ankit Jha, Enrico Fini, Mainak Singha, Elisa Ricci, and Biplab Banerjee. Stylip: Multi-scale style-conditioned prompt learning for clip-based domain generalization. In *Proceedings of the IEEE/CVF Winter Conference on Applications of Computer Vision*, pages 5542–5552, 2024. 1
- [2] Lukas Bossard, Matthieu Guillaumin, and Luc Van Gool. Food-101—mining discriminative components with random forests. In *European Conference on Computer Vision*, pages 446–461. Springer, 2014. 6
- [3] Adrian Bulat and Georgios Tzimiropoulos. LASP: Text-to-text optimization for language-aware soft prompting of vision & language models. In *Proceedings of the IEEE/CVF Conference on Computer Vision and Pattern Recognition*, pages 23232–23241, 2023. 1
- [4] Guangyi Chen, Weiran Yao, Xiangchen Song, Xinyue Li, Yongming Rao, and Kun Zhang. PLOT: Prompt learning with optimal transport for vision-language models. *arXiv preprint arXiv:2210.01253*, 2022. 2
- [5] Hyeong Kyu Choi, Joonmyung Choi, and Hyunwoo J Kim. TokenMixup: Efficient attention-guided token-level data augmentation for transformers. *Advances in Neural Information Processing Systems*, 35:14224–14235, 2022. 3
- [6] Mircea Cimpoi, Subhansu Maji, Iasonas Kokkinos, Sammy Mohamed, and Andrea Vedaldi. Describing textures in the wild. In *Proceedings of the IEEE/CVF Conference on Computer Vision and Pattern Recognition*, pages 3606–3613, 2014. 6
- [7] Ekin D Cubuk, Barret Zoph, Jonathon Shlens, and Quoc V Le. RandAugment: Practical automated data augmentation with a reduced search space. In *Proceedings of the IEEE/CVF Conference on Computer Vision and Pattern Recognition Workshops*, pages 702–703, 2020. 2, 4, 8
- [8] Jia Deng, Wei Dong, Richard Socher, Li-Jia Li, Kai Li, and Li Fei-Fei. ImageNet: A large-scale hierarchical image database. In *Proceedings of the IEEE/CVF Conference on Computer Vision and Pattern Recognition*, pages 248–255. Ieee, 2009. 6, 7
- [9] Mohammad Mahdi Derakhshani, Enrique Sanchez, Adrian Bulat, Victor G Turrissi da Costa, Cees GM Snoek, Georgios Tzimiropoulos, and Brais Martinez. Bayesian prompt learning for image-language model generalization. In *Proceedings of the IEEE/CVF International Conference on Computer Vision*, pages 15237–15246, 2023. 2
- [10] Jian Ding, Nan Xue, Gui-Song Xia, and Dengxin Dai. Decoupling zero-shot semantic segmentation. In *Proceedings of the IEEE/CVF Conference on Computer Vision and Pattern Recognition*, pages 11583–11592, 2022. 1
- [11] Li Fei-Fei, Rob Fergus, and Pietro Perona. Learning generative visual models from few training examples: An incremental bayesian approach tested on 101 object categories. In *Proceedings of the IEEE/CVF Conference on Computer Vision and Pattern Recognition Workshops*, pages 178–178. IEEE, 2004. 6
- [12] Chengjian Feng, Yujie Zhong, Zequn Jie, Xiangxiang Chu, Haibing Ren, Xiaolin Wei, Weidi Xie, and Lin Ma. Prompt-Det: Towards open-vocabulary detection using uncurated images. In *European Conference on Computer Vision*, pages 701–717. Springer, 2022. 1
- [13] Yuqian Fu, Yu Xie, Yanwei Fu, and Yu-Gang Jiang. StyleAdv: Meta style adversarial training for cross-domain few-shot learning. In *Proceedings of the IEEE/CVF Conference on Computer Vision and Pattern Recognition*, pages 24575–24584, 2023. 4
- [14] Peng Gao, Shijie Geng, Renrui Zhang, Teli Ma, Rongyao Fang, Yongfeng Zhang, Hongsheng Li, and Yu Qiao. CLIP-adapter: Better vision-language models with feature adapters. *International Journal of Computer Vision*, 132(2):581–595, 2024. 1
- [15] Wenbin He, Suphanut Jamonnak, Liang Gou, and Liu Ren. CLIP-S4: Language-guided self-supervised semantic segmentation. In *Proceedings of the IEEE/CVF Conference on Computer Vision and Pattern Recognition*, pages 11207–11216, 2023. 1
- [16] Patrick Helber, Benjamin Bischke, Andreas Dengel, and Damian Borth. EuroSAT: A novel dataset and deep learning benchmark for land use and land cover classification. *IEEE Journal of Selected Topics in Applied Earth Observations and Remote Sensing*, 12(7):2217–2226, 2019. 6
- [17] Dan Hendrycks, Steven Basart, Norman Mu, Saurav Kadavath, Frank Wang, Evan Dorundo, Rahul Desai, Tyler Zhu, Samyak Parajuli, Mike Guo, et al. The many faces of robustness: A critical analysis of out-of-distribution generalization. In *Proceedings of the IEEE/CVF International Conference on Computer Vision*, pages 8340–8349, 2021. 6
- [18] Dan Hendrycks, Kevin Zhao, Steven Basart, Jacob Steinhardt, and Dawn Song. Natural adversarial examples. In *Proceedings of the IEEE/CVF Conference on Computer Vision and Pattern Recognition*, pages 15262–15271, 2021. 6
- [19] Minui Hong, Jinwoo Choi, and Gunhee Kim. StyleMix: Separating content and style for enhanced data augmentation. In *Proceedings of the IEEE/CVF Conference on Computer Vision and Pattern Recognition*, pages 14862–14870, 2021. 2, 4
- [20] Xun Huang and Serge Belongie. Arbitrary style transfer in real-time with adaptive instance normalization. In *Proceedings of the IEEE/CVF International Conference on Computer Vision*, pages 1501–1510, 2017. 4
- [21] Chao Jia, Yinfei Yang, Ye Xia, Yi-Ting Chen, Zarana Parekh, Hieu Pham, Quoc Le, Yun-Hsuan Sung, Zhen Li, and Tom Duerig. Scaling up visual and vision-language representation learning with noisy text supervision. In *International Conference on Machine Learning*, pages 4904–4916. PMLR, 2021. 2
- [22] Muhammad Uzair Khattak, Hanoona Rasheed, Muhammad Maaz, Salman Khan, and Fahad Shahbaz Khan. MaPLe: Multi-modal prompt learning. In *Proceedings of the IEEE/CVF Conference on Computer Vision and Pattern Recognition*, pages 19113–19122, 2023. 1, 2, 3, 6, 7, 8
- [23] Muhammad Uzair Khattak, Syed Talal Wasim, Muzammal Naseer, Salman Khan, Ming-Hsuan Yang, and Fahad Shahbaz Khan. Self-regulating prompts: Foundational model adaptation without forgetting. In *Proceedings of the*

- IEEE/CVF International Conference on Computer Vision*, pages 15190–15200, 2023. 6, 7, 8
- [24] Konwoo Kim, Michael Laskin, Igor Mordatch, and Deepak Pathak. How to adapt your large-scale vision-and-language model. 2021. 1
- [25] Jonathan Krause, Michael Stark, Jia Deng, and Li Fei-Fei. 3D object representations for fine-grained categorization. In *Proceedings of the IEEE/CVF International Conference on Computer Vision Workshops*, pages 554–561, 2013. 6
- [26] Kyungmoon Lee, Sungyeon Kim, and Suha Kwak. Cross-domain ensemble distillation for domain generalization. In *European Conference on Computer Vision*, pages 1–20. Springer, 2022. 3
- [27] Ilya Loshchilov and Frank Hutter. Decoupled weight decay regularization. *arXiv preprint arXiv:1711.05101*, 2017. 3
- [28] Yuning Lu, Jianzhuang Liu, Yonggang Zhang, Yajing Liu, and Xinmei Tian. Prompt distribution learning. In *Proceedings of the IEEE/CVF Conference on Computer Vision and Pattern Recognition*, pages 5206–5215, 2022. 2, 6, 7
- [29] Subhransu Maji, Esa Rahtu, Juho Kannala, Matthew Blaschko, and Andrea Vedaldi. Fine-grained visual classification of aircraft. *arXiv preprint arXiv:1306.5151*, 2013. 6
- [30] Muhammad Ferjad Naeem, Yongqin Xian, Luc V Gool, and Federico Tombari. I2DFormer: Learning image to document attention for zero-shot image classification. *Advances in Neural Information Processing Systems*, 35:12283–12294, 2022. 2
- [31] Maria-Elena Nilsback and Andrew Zisserman. Automated flower classification over a large number of classes. In *2008 Sixth Indian Conference on Computer Vision, Graphics & Image Processing*, pages 722–729. IEEE, 2008. 6
- [32] Omkar M Parkhi, Andrea Vedaldi, Andrew Zisserman, and CV Jawahar. Cats and dogs. In *Proceedings of the IEEE/CVF Conference on Computer Vision and Pattern Recognition*, pages 3498–3505. IEEE, 2012. 6
- [33] Alec Radford, Jong Wook Kim, Chris Hallacy, Aditya Ramesh, Gabriel Goh, Sandhini Agarwal, Girish Sastry, Amanda Askell, Pamela Mishkin, Jack Clark, et al. Learning transferable visual models from natural language supervision. In *International Conference on Machine Learning*, pages 8748–8763. PMLR, 2021. 1, 2, 3, 6, 7
- [34] Yongming Rao, Wenliang Zhao, Guangyi Chen, Yansong Tang, Zheng Zhu, Guan Huang, Jie Zhou, and Jiwen Lu. DenseCLIP: Language-guided dense prediction with context-aware prompting. In *Proceedings of the IEEE/CVF Conference on Computer Vision and Pattern Recognition*, pages 18082–18091, 2022. 1
- [35] Hanoona Rasheed, Muhammad Uzair Khattak, Muhammad Maaz, Salman Khan, and Fahad Shahbaz Khan. Fine-tuned CLIP models are efficient video learners. In *Proceedings of the IEEE/CVF Conference on Computer Vision and Pattern Recognition*, pages 6545–6554, 2023. 3, 6
- [36] Benjamin Recht, Rebecca Roelofs, Ludwig Schmidt, and Vaishaal Shankar. Do ImageNet classifiers generalize to ImageNet? In *International Conference on Machine Learning*, pages 5389–5400. PMLR, 2019. 6
- [37] Shuvendu Roy and Ali Etemad. Consistency-guided prompt learning for vision-language models. *arXiv preprint arXiv:2306.01195*, 2023. 3, 6, 7, 8
- [38] Khurram Soomro, Amir Roshan Zamir, and Mubarak Shah. UCF101: A dataset of 101 human actions classes from videos in the wild. *arXiv preprint arXiv:1212.0402*, 2012. 6
- [39] Nitish Srivastava, Geoffrey Hinton, Alex Krizhevsky, Ilya Sutskever, and Ruslan Salakhutdinov. Dropout: a simple way to prevent neural networks from overfitting. *The Journal of Machine Learning Research*, 15(1):1929–1958, 2014. 3
- [40] Maria Tsimpoukelli, Jacob L Menick, Serkan Cabi, SM Eslami, Oriol Vinyals, and Felix Hill. Multimodal few-shot learning with frozen language models. *Advances in Neural Information Processing Systems*, 34:200–212, 2021. 1
- [41] SS Vallender. Calculation of the Wasserstein distance between probability distributions on the line. *Theory of Probability & Its Applications*, 18(4):784–786, 1974. 4
- [42] Haohan Wang, Songwei Ge, Zachary Lipton, and Eric P Xing. Learning robust global representations by penalizing local predictive power. *Advances in Neural Information Processing Systems*, 32, 2019. 6
- [43] Yue Wang, Lei Qi, Yinghuan Shi, and Yang Gao. Feature-based style randomization for domain generalization. *IEEE Transactions on Circuits and Systems for Video Technology*, 32(8):5495–5509, 2022. 1
- [44] Jianxiong Xiao, James Hays, Krista A Ehinger, Aude Oliva, and Antonio Torralba. SUN database: Large-scale scene recognition from abbey to zoo. In *Proceedings of the IEEE/CVF Conference on Computer Vision and Pattern Recognition*, pages 3485–3492. IEEE, 2010. 6
- [45] Lingxiao Yang, Ru-Yuan Zhang, Yanchen Wang, and Xiaohua Xie. MMA: Multi-modal adapter for vision-language models. In *Proceedings of the IEEE/CVF Conference on Computer Vision and Pattern Recognition*, pages 23826–23837, 2024. 6, 7, 8
- [46] Lewei Yao, Runhui Huang, Lu Hou, Guansong Lu, Minzhe Niu, Hang Xu, Xiaodan Liang, Zhenguo Li, Xin Jiang, and Chunjing Xu. FILIP: Fine-grained interactive language-image pre-training. *arXiv preprint arXiv:2111.07783*, 2021. 2
- [47] Jure Zbontar, Li Jing, Ishan Misra, Yann LeCun, and Stéphane Deny. Barlow Twins: Self-supervised learning via redundancy reduction. In *International conference on Machine Learning*, pages 12310–12320. PMLR, 2021. 5
- [48] Kaiyang Zhou, Jingkang Yang, Chen Change Loy, and Ziwei Liu. Conditional prompt learning for vision-language models. In *Proceedings of the IEEE/CVF Conference on Computer Vision and Pattern Recognition*, pages 16816–16825, 2022. 1, 2, 3, 6, 7, 8
- [49] Kaiyang Zhou, Jingkang Yang, Chen Change Loy, and Ziwei Liu. Learning to prompt for vision-language models. *International Journal of Computer Vision*, 130(9):2337–2348, 2022. 1, 3, 6, 7, 8
- [50] Kaiyang Zhou, Yongxin Yang, Yu Qiao, and Tao Xiang. Domain generalization with MixStyle. *arXiv preprint arXiv:2104.02008*, 2021. 1, 4, 8